

Phase Diagram for Quantum Hall Bilayers at $\nu = 1$

D. N. Sheng,¹ Leon Balents,² and Ziqiang Wang³

¹*Department of Physics and Astronomy, California State University, Northridge, CA 91330*

²*Department of Physics, University of California, Santa Barbara, CA 93106*

³*Department of Physics, Boston College, Chestnut Hill, MA 02467*

(Dated: February 7, 2020)

We present a phase diagram for a double quantum well bilayer electron gas in the quantum Hall regime at total filling factor $\nu = 1$, based on exact numerical calculations of the topological Chern number matrix and the (inter-layer) superfluid density. We find three phases: a quantized Hall state with pseudo-spin superfluidity, a quantized Hall state with pseudo-spin “gauge-glass” order, and a decoupled composite Fermi liquid. Comparison with experiments provides a consistent explanation of the observed quantum Hall plateau, Hall drag plateau and vanishing Hall drag resistance, as well as the zero-bias conductance peak effect, and suggests some interesting points to pursue experimentally.

PACS numbers: 73.21.-b, 11.15.-q, 73.43.Lp

The coexistence of an incompressible integer quantum Hall effect (IQHE) state and interlayer superfluidity has been established through a series of experimental and theoretical works on bilayer two dimensional electron systems at a total electron filling number $\nu = 1$ ^{1,2,3,4}. Such an IQHE is a consequence of the strong Coulomb interactions, which lead to a charge gap at $\nu = 1$. Denoting the layer index as pseudospin “up” and “down”, the ground state is a quantum ferromagnet with spontaneous interlayer phase coherence^{5,6}, which exhibits superfluidity in the zero layer separation limit, $d = 0$. On the other hand, in the $d \rightarrow \infty$ limit, the two layers are decoupled, each comprising a compressible composite fermion liquid at $\nu = 1/2$. The nature of the phases and transitions^{7,8,9,10,11} between these two limits has attracted many recent studies. A generalized pseudospin description suggests a first order transition⁸ at which the pseudospin order vanishes upon increasing d . The relation of the loss of ferromagnetism with the disappearance of the IQHE remains unclear, and indeed several scenarios in which the ferromagnetism and IQHE do not vanish simultaneously have also been proposed based on the Chern-Simons mean-field theory⁹. Furthermore, in real samples with impurities, a first order transition is believed to be impossible on general grounds¹². A consistent picture for the phase transitions is still absent.

Fundamentally, the distinct phases of the system at $T = 0$ are characterized by their topological order and/or broken symmetries. Experimentally, these are predominantly reflected in electrical transport coefficients, particularly the Hall conductance. Due to the lack of exact solutions (except at $d = 0$ without impurities), the ground state phases and transport properties have mainly been discussed based on effective theories^{5,7,9}. Exact numerical calculations for these systems have been done in the absence of random disorder potential^{10,11}, which cannot provide direct information about the transport. In this letter, we report the first finite-size exact calculations of transport properties for such a system in the presence of random impurities, by obtaining the topological Chern

number matrix of the many-body wavefunction and the superfluid density of the ground state.

The Chern number^{13,14} is a unique integer topological invariant associated with a wavefunction, and can be used to distinguish different quantum Hall states. Physically, the Chern number equals the boundary condition averaged Hall conductance (in units of e^2/h), so an IQHE state is expected to display a fixed non-zero integer Chern number independent of disorder configurations. A state with a non-quantized Hall conductance instead displays a random integer Chern number intrinsically fluctuating with different disorder configurations or other external parameters. Such states are generally expected to be critical or fluid in nature, since a nonzero current^{14,15} necessarily exists in the bulk to destroy the exact quantization of Hall conductance. Thus the distribution of Chern numbers over samples also reveals the extended or localized character of the state.

Numerical calculations of the Chern number have up to now only been carried out from single-particle wavefunctions in non-interacting systems^{14,15}. The Chern number of a many-body wavefunction is, nevertheless, well-defined, albeit difficult to calculate. We have developed a new approach to obtain the exact Chern number by numerically evaluating the Berry phase of the many-body wavefunction upon changing boundary phases adiabatically¹⁶. In the present bilayer system the topological Chern numbers form a 2×2 matrix related to the topological ordering of the system¹⁷, which determines the charge and spin (we will refer pseudospin as spin) Hall conductances (as well as the Hall drag, which is the difference of the two).

Our main results can be summarized as a numerical phase diagram (see Fig. 1) in the $d - W$ plane (W is the disorder strength) with three distinguishable phases. Phase I is the usual bilayer ferromagnet, embodying coexistence of the $\nu = 1$ IQHE and inter-layer superfluidity, occurring at small d and W . At relatively strong W but small d regime, the superfluid state will first undergo a phase transition to a “gauge glass” (phase II), in

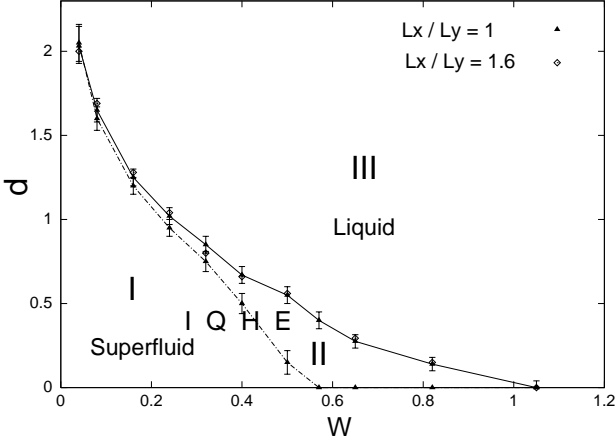


FIG. 1: The solid line is the critical layer separation d_c vs. W , which separates the IQHE plateau (phase I and II) from the composite Fermi liquid state (phase III). The dashed line is the critical d_s vs. W , which separates the superfluid state (phase I) from the gauge glass state (phase II).

which n_s vanishes due to strong phase frustration. Both phases I and II have the same Chern number matrix: a uniquely quantized charge Chern number $C^c = 1$ and a random spin Chern number, which result in nonzero Hall drag conductance. In phase I, spin superfluidity implies that the full spin resistivity tensor and hence ρ_{xy}^s vanishes below the Kosterlitz-Thouless temperature, so we expect quantization of the Hall drag resistance, $\rho_{xy}^d = \rho_{xy}^c - \rho_{xy}^s = h/e^2$ with exponentially small thermally activated corrections at low temperature. Phase II, despite having the same Chern number matrix as phase I, has a different behavior of the spin resistivity, since the average n_s vanishes. Conventional theory for the gauge glass carried over to this problem suggests⁵ $\rho_{xy}^s \sim \rho_{xx}^s$ are exponentially small but non-zero at any $T > 0$ and vanish only at $T = 0$, leading to a weaker quantization of the Hall drag resistance. With the increase of d or W , phase II undergoes a transition to the compressible Fermi liquid (phase III). Phase III can be understood from the large d limit of decoupled layers. It is a metallic state, characterized by zero drag conductance and a finite diagonal longitudinal conductance. These results provide a consistent understanding for the existing experiments (see below).

In the presence of a strong magnetic field, the Hamiltonian, projected onto the lowest Landau level, for a double layer two-dimensional electron gas can be written as:

$$H = \sum_{i < j, \alpha, \beta} \sum_{\mathbf{q} \neq 0} e^{-q^2/2} V_{\alpha, \beta}(q) e^{i\mathbf{q} \cdot (\mathbf{R}_i^\alpha - \mathbf{R}_j^\beta)} + \sum_{i, \alpha} \sum_{\mathbf{q} \neq 0} e^{-q^2/4} V_{\text{imp}}^\alpha(q) e^{i\mathbf{q} \cdot \mathbf{R}_i^\alpha} \quad (1)$$

where \mathbf{R}_i^α is the coordinate of the i -th electron in layer α ($\alpha = 1, -1$). $V_{\alpha, \beta}(q) = 2\pi e^2 / (\epsilon q L_x L_y) \times \exp(-qd\delta_{\alpha, -\beta})$, is the Coulomb potential. $V_{\text{imp}}^\alpha(q)$ is the impurity potential generated according to the correlation relation $\langle V_{\text{imp}}^\alpha(q) V_{\text{imp}}^\beta(-q') \rangle = \frac{W^2}{L_x L_y} \delta_{\alpha, \beta} \delta_{q, q'}$, which corresponds

to $\langle V_{\text{imp}}^\alpha(\mathbf{r}) V_{\text{imp}}^\beta(\mathbf{r}') \rangle = W^2 \delta_{\alpha, \beta} \delta(\mathbf{r} - \mathbf{r}')$ in real space, where W is the strength of the disorder. We set the magnetic length $\ell = 1$ and the interaction strength $e^2/\epsilon\ell = 1$ for convenience. We impose the generalized boundary conditions: $T^\alpha(\mathbf{L}_j)|\Phi\rangle = e^{i\theta_j^\alpha}|\Phi\rangle$ ($j = x, y$), to the finite size double layer system, each in an $L_x \times L_y$ rectangular cell with an integer number of flux quanta $N_s = L_x L_y / 2\pi$. $T^\alpha(\mathbf{r})$ is the many-body magnetic translation operator. The tunneling term is not considered here in order to study the interesting limit where the correlation between two layers is purely due to Coulomb interaction. We consider up to $N_e = 12$ electrons at filling number $\nu = N_e/N_s = 1$, spanning a Hilbert space of size $N_{\text{basis}} = 853776$.

Through a unitary transformation $\Psi = \exp[-i \sum_{i=1}^{N_e} \sum_{\alpha} (\frac{\theta_x^\alpha}{L_x} x_i^\alpha + \frac{\theta_y^\alpha}{L_y} y_i^\alpha)] \Phi$, the topological Chern number^{13,15} can be calculated as:

$$C^{\alpha, \beta} = \frac{i}{4\pi} \oint d\theta_j \{ \langle \Psi | \frac{\partial \Psi}{\partial \theta_j} \rangle - \langle \frac{\partial \Psi}{\partial \theta_j} | \Psi \rangle \}. \quad (2)$$

where θ_j has layer index α and β with $\theta_j = \theta_x^\alpha, \theta_y^\beta$. With $\alpha, \beta = -1, 1$, $C^{\alpha, \beta}$ forms a 2×2 matrix. The closed path integral is along the phase boundary of the $2\pi \times 2\pi$ unit cell. If common or opposite boundary phases are opposed on the two layers, then one obtains charge and spin Chern number, $C^{c, s}$, which is related to the boundary phase averaged charge and spin Hall conductances $\sigma_{xy}^{c, s} = C^{c, s} \frac{e^2}{h}$, respectively. We separate the phase space into a mesh of 64-200 squares. By repeatedly calculating wavefunctions at all nodes of the mesh using Lanczos method, we determine the integer Chern number for the many-body state in each disorder configuration.

We first consider the charge Chern number C^c as a function of d . At a weak disorder strength $W = 0.16$ and $d < 1$, we find $C^c = 1$ for all disorder samples at $N_e = 6, 8, 10, 11$ and 12 (20 samples for $N_e = 12$ and 1000 for $N_e = 6$). Hence the corresponding ground state displays the IQHE with total (charge) Hall conductance $\sigma_{xy}^c = \frac{e^2}{h}$. As we further increase d , a strong fluctuation of the Chern number takes place at $d \sim 1.1 - 1.3$, which are caused by level crossings upon tuning the boundary phases and disorder. The persistence of the crossing of low energy states at particular values of d, W is a signature of a quantum phase transition, and is associated with the collapse of the mobility gap. Thus the mobility of the state in the charge channel is tied to the fluctuations of C^c ^{14,15}, motivating us to define $\rho_{\text{ext}} = P(C^c \neq 1)$ (the probability of finding $C^c \neq 1$) as a characterization of the extensiveness of the many-body state. If ρ_{ext} extrapolates to a nonzero value in the thermodynamic limit, it represents a fluid phase which can carry current in the bulk to spoil the exact quantization of σ_{xy}^c .

To determine the critical d_c for the $\nu = 1$ IQHE to metal transition, we plot ρ_{ext} as a function of d at $W = 0.16$, $N_e = 6, 10$ and 11 in Fig.2. ρ_{ext} always increases rapidly around $d \sim 1.1 - 1.3$ and saturates to 0.5 at larger d . In the same figure, we plot $\Delta\rho_{\text{ext}}/\Delta d$ ($\Delta d = 0.05$) as

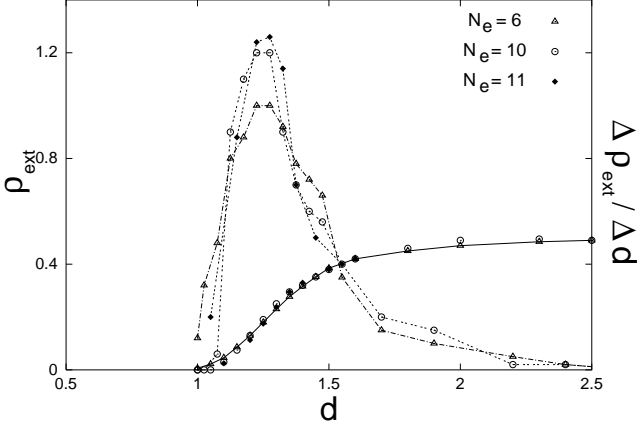


FIG. 2: The effective charge mobility ρ_{ext} at $W = 0.16$, defined as the ratio of the number of samples with $C^c \neq 1$ and the total number of samples, as a function of d at $N_e = 6, 10$ and 11 . $\Delta\rho_{ext}/\Delta d$ vs. d is also shown.

a function of d . Around $d = 1.25$, there is always a very strong peak growing with N_e . We determine the critical layer separation d_c ($= 1.25 \pm 0.05$ for $W = 0.16$) for the IQHE to metal transition by the location of the maximum of this peak for each W . A step jump of ρ_{ext} is expected for such a transition in the thermodynamic limit.

The critical d_c as a function of W determined in this manner is indicated in Fig. 1 by the solid line. The d_c for two aspect ratios ($L_x/L_y = 1$ and 1.6) agree well with each other, demonstrating the smallness of overall finite size effects. At $W \rightarrow 0$, d_c saturates to around $d_c = 2.2 \pm 0.2$ with relatively large error bars due to increasing finite-size effects at very weak W (at $W = 0.04$, $d_c = 2.02 \pm 0.13$). We note that studies based on the local ferromagnetic moment m_{FM} for weak disorder will tend to underestimate d_c , due to a large reduction of m_{FM} by low energy states mixing around $d \approx 1.5$, which, however, does not affect the Chern number.

More information on the nature of spin sector can be obtained by tuning the boundary conditions in two layers according to $\theta_t = \theta_x^1 = -\theta_x^{-1}$. The energies of the lowest two states E_g and E_1 change significantly with θ_t , with variations of the order of the level spacing. At small d and W , E_g first increases as a quadratic function of θ_t until it is energetically favorable for a vortex (through the hole in the torus encircled by the x axis) to enter the system, a typical feature of a superfluid state. The disorder averaged superfluid density can be calculated as $n_s = \frac{1}{2} \langle \frac{\partial^2 E_g}{\partial \theta_t^2} \bigg|_{\theta_t=0} \rangle^{18}$.

In Fig. 3, n_s is plotted as a function of d at $W = 0.16$ for $N_e = 6, 8, 10$ and 12 . The overall behavior agrees with the generalized mean-field calculation for pure system (our definition of n_s is twice that of Ref. 8). Naturally, n_s reduces with increasing d , and we define the boundary of the superfluid state d_s by $n_s = 0$, e.g. $d_s = 1.2$ for $W = 0.16$ shown here. The critical d_s is also shown in Fig. 1 as the dashed line. In the strong W case, d_s becomes obviously smaller than d_c , indicating a superfluid state (phase I) to phase II tran-

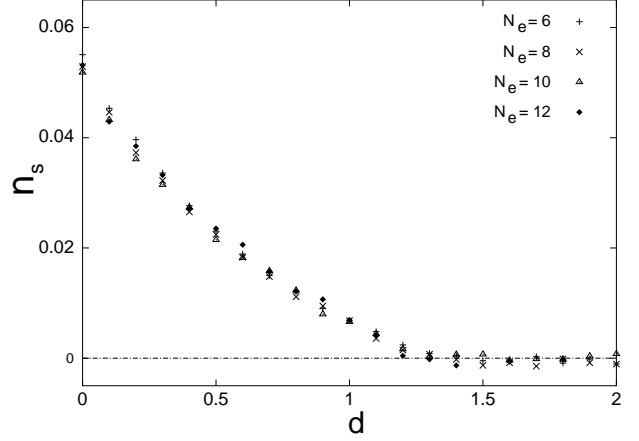


FIG. 3: The superfluid density n_s vs. d at $W = 0.16$. At the transition point $d_s = 1.2$, $n_s \rightarrow 0$.

sition inside the IQHE regime. In phase II, the averaged superfluid density vanishes, due principally to phase frustration: $E_g(\theta_t)$ still depends strongly upon θ_t with positive or negative curvatures depending on disorder realizations. We postulate hence that the spin sector in phase II behaves as a gauge or vortex glass¹⁹, with Edwards-Anderson magnetic order and algebraic stiffness $\langle |E_g(\theta_t = \pi/2) - E_g(\theta_t = 0)| \rangle \sim L^{-|\Theta|}$, as proposed for $\nu = 1$ bilayers in Ref. 5.

Further evidence that phase II is not a spin insulator is obtained from the spin Chern number C^s , determined by imposing opposite boundary phases to both layers. We find that C^s fluctuates (around 1) throughout the $d - W$ plane, implying fluidity of the spin sector and a non-quantized spin Hall conductance. This rules out a spin insulator for phase II, favoring the interpretation as a gauge glass. In both phase I and II, the Hall drag conductance $\sigma_{xy}^{1,-1} + \sigma_{xy}^{-1,1} = \frac{1}{2}(\sigma_{xy}^c - \sigma_{xy}^s) = (C^c - C^s)\frac{e^2}{2h}$, is also non-quantized and non-zero, which is a consequence of the coupling between two layers. At the phase boundary for the IQHE ($d = d_c$), we find that the nondiagonal Chern number $C^{1,-1} = C^{-1,1} = 0$ and the drag Hall conductance drops to zero, indicating that the spin sector is also involved in the phase transition at $d = d_c$. At this gauge glass to composite Fermi liquid critical point, we expect the spin correlations go from (Edwards-Anderson-)superfluid to metallic.

To reveal the charge plateau, we calculate σ_{xy}^c as a function of ν . Shown in Fig. 4, at $W = 0.16$ and $d = 0.8$, we observe an exact quantized plateau between $\nu = 11/12 = 0.91$ and $\nu = 13/12 = 1.09$, with $\rho_{ext} = 0$ corresponding to a finite mobility gap. The plateau width is usually smaller or around $\Delta\nu = 0.2$ depending on W , in good agreement with experiments²⁰. In contrast to the plateau in charge channel around $\nu = 1$, the spin Chern number fluctuates with different disorder configurations, as shown in the inset of Fig. 4.

We conclude with some comparison to experiments. Both phases I and II exhibit the IQHE in the charge channel, i.e. $\rho_{xy}^c = h/e^2$ and $\rho_{xx}^c = 0$ at zero temperature, and we expect activated corrections at $T > 0$. The spin Chern

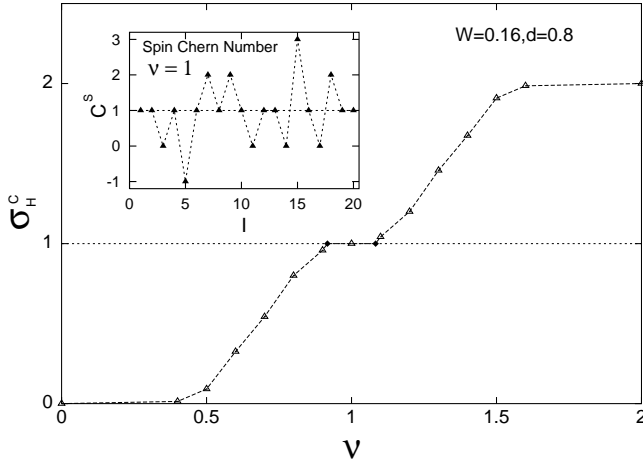


FIG. 4: The charge Hall conductance σ_{xy}^c (in units of e^2/h) vs. filling number $\nu = N_e/N_s$. In the inset, the random spin Chern number C^s vs. disorder configuration I for 20 samples at $\nu = 1$. $W = 0.16$ and $d = 0.8$ (in phase I) for both data.

number is random and fluctuating, which gives rise to a nonquantized spin conductance. The exact quantized Hall plateau (for the charge) has been observed by several experimental groups^{1,20} with a critical $d_c^{exp} = 1.8$, corresponding to the regime of very weak $W \approx 0.07$ in our phase diagram. In this regime, the width of phase II is extremely narrow if non-zero, and the Hall plateau phase at $d < d_c$ observed experimentally therefore corresponds to phase I. As a true two-dimensional superfluid, it is expected to exhibit anomalous properties, e.g. divergent σ_{xx}^s even at non-zero temperatures below the Kosterlitz-Thouless temperature, $T < T_{KT}$. The experimentally observed zero-bias tunneling conductance peak below a characteristic temperature⁴ is a direct reflection of the associated off-diagonal order in the spin channel. Furthermore, the divergent spin conductivity implies that

the full spin resistivity tensor must vanish, $\rho_{xx}^s = \rho_{xy}^s = 0$ for $T < T_{KT}$. At $T = 0$, the IQHE then implies quantized Hall drag $\rho_{xy}^d = \rho_{xy}^c - \rho_{xy}^s = h/e^2$ and vanishing longitudinal drag, $\rho_{xx}^d = \rho_{xx}^c - \rho_{xx}^s = 0$, in agreement with experiments²⁰. While the quantization of Hall drag is expected to be violated for $T > 0$ by activated processes contributing to ρ_{xx}^c , the theory predicts that the spin Hall resistivity, should vanish even at non-zero temperature for $T < T_{KT}$, which would be interesting to explore experimentally. For $d > d_c$, in phase III, we obtain $C^{1,-1} = C^{-1,1} = 0$ numerically, signaling the decoupling of two layers. As a consequence, the drag conductance and resistance reduce to zero at $T = 0$, which also agrees with the experiment²⁰ at larger d ($d > d_c^{exp}$). Lastly, for the relatively pure sample used in Ref.20, phase I is directly neighboring phase III which results in $\rho_{xx}^d \neq 0$ only along the phase transition line $d = d_c$ at very low temperature, a property again observed experimentally²⁰. For more disordered samples at intermediate d , phase II (gauge glass) intervenes. While we expect this phase exhibits the same transport coefficients as phase I at $T = 0$, it has no associated Kosterlitz-Thouless transition. This implies that ρ_{xy}^s, ρ_{xx}^s are generally non-zero for $T > 0$ in this range, and probably that ρ_{xx}^d is enhanced at low but non-zero temperatures. We leave a more detailed investigation of the gauge glass to a future study.

We would like to acknowledge helpful discussions with Jim Eisenstein, Matthew Fisher, Dung-Hai Lee, and Z. Y. Weng. This work was supported by ACS-PRF # 36965-AC5 and Research Corporation Award CC5643, the NSF through grants DMR-00116566 (DNS), DMR-9985255, the Sloan and Packard foundations (LB), and DOE grant DE-FG02-99ER45747 (ZW). DNS would like to thank the hospitality and support from the KITP at Santa Barbara.

- ¹ J.P.Eisenstein *et al.* Phys. Rev. Lett. **68**, 1383 (1992).
- ² X. -G. Wen and A. Zee, Phys. Rev. Lett. **69**, 1811 (1992).
- ³ S. Q. Murphy *et al.*, Phys. Rev. Lett. **72**, 728 (1994); K. Moon *et al.*, Phys. Rev. B **51**, 5138 (1995); K. Yang *et al.*, *ibid.* **54**, 11644 (1996).
- ⁴ I. B. Spieman *et al.*, Phys. Rev. Lett. **84**, 5808 (2000).
- ⁵ L. Balents and L. Radzihovsky, Phys. Rev. Lett. **86**, 1825 (2001).
- ⁶ S. Stern *et al.*, Phys. Rev. Lett. **86**, 1829 (2001); M. Fogler and F. Wilczek, *ibid.* **86**, 1833 (2001).
- ⁷ A. Stern and B. I. Halperin, Phys. Rev. Lett. **88**, 106801 (2002).
- ⁸ Y. N. Joglekar and A. H. MacDonald, Phys. Rev. B **64**, 155315 (2001).
- ⁹ Y. B. Kim *et al.*, Phys. Rev. B **63**, 205315 (2001); M. Veillette, L. Balents and M. P. A. Fisher, *ibid.* **66**, 155401 (2002).
- ¹⁰ J. Schliemann, S. M. Girvin, and A. H. MacDonald, Phys. Rev. Lett. **86**, 1849 (2001).
- ¹¹ F. D. M. Haldane and E. H. Rezayi, Phys. Rev.

- Let. **60**, 956 (1988); K. Nomura and D. Yoshioka, cond-mat/0204461.
- ¹² Y. Imry and M. Wortis, Phys. Rev. B **19**, 3580 (1979); M. Aizenman and J. Wehr, Phys. Rev. Lett. **62**, 2503 (1989).
- ¹³ Q. Niu, D.J. Thouless and Y.S. Wu, Phys. Rev. B **23**, 5632 (1985); D.J. Thouless *et al.*, Phys. Rev. Lett. **49**, 405 (1982).
- ¹⁴ D. P. Arovas *et al.*, Phys. Rev. Lett. **60**, 619 (1988); Y. Huo, and R.N. Bhatt, *ibid.* **68**, 1375 (1992).
- ¹⁵ D. N. Sheng and Z. Y. Weng, Phys. Rev. Lett. **75** (1995) 2388; *ibid.* **78**, 318 (1997); Phys. Rev. B **54**, R11070 (1996); Yang K. and Bhatt R. N., *ibid.* **55**, (1997) R1922.
- ¹⁶ D. N. Sheng, X. Wan, E. H. Rezayi, Kun Yang, R. N. Bhatt and F. D. M. Haldane, to be published.
- ¹⁷ X. G. Wen and A. Zee, Phys. Rev. B **44**, 274 (1991).
- ¹⁸ B. S. Shastry and B. Sutherland, Phys. Rev. Lett. **65**, 243 (1990).
- ¹⁹ Matthew P. A. Fisher, Phys. Rev. Lett. **62**, 1415 (1990).
- ²⁰ M. Kellogg *et al.*, Phys. Rev. Lett. **88**, 126804 (2002).